Blocking PSD-93-CX3CL1 Interaction Promotes the Phenotypic Transformation of Microglia During Acute Ischemic Stroke

qingxiu zhang (zhangqingxiu@163.com)
Nanjing University Medical School Affiliated Nanjing Drum Tower Hospital https://orcid.org/0000-0001-5285-2908

xiaowei cao
Nanjing University Medical School Affiliated Nanjing Drum Tower Hospital

hui yang
Nanjing University Medical School Affiliated Nanjing Drum Tower Hospital

xiaomei Liu
Xuzhou Medical University

shiying Lou
Nanjing University Medical School Affiliated Nanjing Drum Tower Hospital

liping kong
Xuzhou Medical University

liangqun rong
Xuzhou Medical University

junjun shan
Xuzhou Medical University

yun xu
Nanjing University Medical School Affiliated Nanjing Drum Tower Hospital

Research

Keywords: PSD-93, CX3CL1, Tat-CX3CL1 (357-395aa), cerebral ischemia-reperfusion, Microglia

Posted Date: July 14th, 2021

DOI: https://doi.org/10.21203/rs.3.rs-687096/v1

Abstract

Background

Postsynaptic density 93 (PSD-93) plays an important role in ischemic brain injury by mediating neurotoxicity and neuroinflammation. Different photypes of microglia perform an important role in ischemic crerbral injury and repair. Blocking the combination of PSD-93 and CX3C chemokine ligand 1 (CX3CL1) is beneficial in acute ischemic stroke, but the underlying mechanism remains unclear.

Methods

Middle cerebral artery occlusion (MCAO) model was established in male C57BL/6 mice. The peptide Tat-CX3CL1 (357-395aa) which disturbing the interaction of PSD-93 and CX3CL1 was used in this study to explore the mechanism of its neuroprotective effect. The production and secretion of cytokines associated with M1 and M2 type of microglia was detected by PCR and ELISA, respectively. Neurologic damage was evaluated by behavior, triphenyl tetrazolium chloride staining, and brain water content. MBP and SMI32 double immunostaining were used to detect white matter injury and double staining for Iba1 and CD68 to assess M1 type microglia polarization.

Results

The cytokines level of M1 phenotype cytokines was increased at 6 h after stroke and peaked at 24 h after perfusion. However, the cytokines level of M2 phenotype was decreased at 6 h and 24 h following reperfusion. The Tat-CX3CL1 (357-395aa) facilitated microglial polarization from M1 type to M2 type by reducing the production of soluble CX3CL1. Furthermore, ADAM17 inhibitor GW280264x could restrain the polarization of microglia from M1 to M2 via reducing soluble CX3CL1 formation. Moreover, Tat-CX3CL1 (357-395aa) attenuated long-term cognitive deficits and improved white matter integrity.

Conclusions

Blocking the binding between CX3CL1 and PSD-93 by Tat-CX3CL1 (357-395aa) could facilitate the functional recovery after ischemic stroke by promoting M1 to M2 microglial polarization transformation. Tat-CX3CL1 (357-395aa) may be a potent agent for ischemic stroke treatment.

Background

Ischemic stroke induces neurotoxicity and neuroinflammation, is a leading cause of death and disability [1-4]. Inflammatory responses induced by microglia polarization exacerbate cerebral infarction [5]. Microglial heterogeneity is of paramount importance for ischemic brain injury, and the polarization of microglia toward M2 phenotype was protective for ischemic stroke [6]. However, the polarization of microglia is highly dependent on environmental signals during cerebral ischemia-reperfusion [7, 8]. Therefore, intervention to promote the microglia to maintain M2 phenotype is a good strategy to achieve functional recovery after stroke.

Traditionally, microglia is considered to be specific tissue-resident macrophages in the central nervous system (CNS) [8, 9]. In response to ischemic stroke, microglial cells initiate the production of pro-inflammatory mediators such as interleukin (IL)-1β, tumor necrosis factor (TNF)-α and IL-6, showing M1 phenotype polarization [10, 11]. In contrast, M2 phenotype microglia plays an anti-inflammatory role by producing anti-inflammatory cytokines including IL-4, IL-10 and transforming growth factor-β (TGF-β) [10, 11]. In recent years, considerable efforts have been devoted to elucidate the role of microglia phenotypic polarization shift in ischemic brain injury [5, 6, 12-14].

Our previous study showed that PSD-93 binds directly to 670-685 amino acid sequence of GTPase-activating protein for Ras (SynGAP) and promotes SynGAP ubiquitination in ischemic brain injury [15]. Knockout of PSD-93 improves neurological deficit by promoting the expression of anti-inflammatory cytokines and inhibiting pro-inflammatory cytokines [16]. Furthermore, we found that PSD-93 interacted with CX3CL1 to mediate neuron-microglia crosstalk and induce neuroinflammation[17]. Using yeast two hybrid and co-immunoprecipitation assay, we identified the binding sites and constructed a small peptide Tat-CX3CL1 (357-395aa) to disturb the combination of PSD-93 and CX3CL1 and attenuate cerebral infarct volume[17], but the underlying mechanism remains elusive.

In this study, we showed that Tat-CX3CL1 (357-395aa) peptide improved functional recovery after ischemic stroke by promoting M2 type microglia polarization. Delivery of Tat-CX3CL1 (357-395aa) inhibited the production of M1 type proinflammatory mediators, facilitated M2 type anti-inflammatory cytokines production and improved the integrity of blood-brain barrier (BBB) after stroke. Furthermore, Tat-CX3CL1 (357-395aa) reduced cerebral infarct volume and improved long-term cognitive function after stroke.

Materials And Methods

Antibodies and Reagents

The sequence of peptide Tat-CX3CL1 (357-395aa) (catalog number: 04010055093, China Peptides, Shanghai, China) was 5-FITC-(Acp) MFAYQSLQGCPRKMAGEMVEGLRYVPRSCGSNS YVLVPV (purity >95%). Primary antibodies were Rabbit polyclonal anti-Iba1 (catalog number: 019-19741, Wako company, Japan), rat monoclonal anti-CD68 (catalog number: ab53444, Abcam company, Cambridge, UK), Rabbit polyclinal to Myelin Basic Protein antibody（catalog number: ab40390, Abcam company, Cambridge, UK）, mouse anti-Neurofilament H (NF-H) (SMI32; catalog number: 801701, BioLegend, San Diego, CA, USA). The secondary antibodies were Alexa Flour cy3 goat anti-rabbit IgG (catalog number: E031620, Earthox, LLC, San Francisco, CA, USA), Alexa Flour 488 donkey anti-rat IgG (catalog number: 21208, Invitrogen), Alexa Flour 488 goat anti-mouse IgG (catalog number: ab150113, Abcam company, Cambridge, UK). ELISA kits were purchased from R&D. GW280264x (catalog number: 555806) was from Medkoo Biosciences.

Animals

C57BL/6 mice (male, 22-26 g weight) were purchased from Pengyue Company (Jinan, Shandong, China), and kept in a 12 h/12 h light-dark cycle with ad libitum food and water. The protocols were approved by Animal Care Committee of Xuzhou Medical University (No. 201702w012), and animal experiments were carried out in accordance with ARRIVE guidelines and the National Institutes of Health guide for the care and use of laboratory animals. Only male mice were used to exclude the effects of estrogen on ischemic injury and stress. Middle cerebral artery occlusion (MCAO) model was established in experimental groups following previous protocol [18]. In the sham operation group, mice received the same surgical procedures without occluding the carotid arteries.

Mice were euthanized by cervical dislocation and the mortality rate after surgery was 8.05%. Among 261 mice used in this study, 26 mice were excluded because of the failure of ischemia induction (5 mice), death (5 mice), cerebral hemorrhage (8 mice), and consciousness disturbance (8 mice).

Tat-CX3CL1 (357-395aa) was diluted with DMSO and administrated into the mice by intracerebroventricular injection. Mice received peptide or DMSO as control before MCAO and at 1d, 2d, and 3d postsurgery (see in supplemental 1). The right cerebral ventricle was selected to inject the peptide or DMSO (from the bregma: anteroposterior-1 mm; lateral 1 mm; depth 2 mm) [17].

Mice were randomly assigned to receive DMSO or ADAM17 inhibitor GW280264x at concentration (0.25μg/μl, 0.5μg/μl, 1.0μg/μl, and 1.5μg/μl) by intranasal administration immediately after MCAO surgery [18, 19] . Five 2-μL drops (total 10 μL) of GW280264x were applied alternately into each nostril with a 2-min interval between drops. Control groups received the same volume of DMSO.

Triphenyl tetrazolium chloride (TTC) staining

TTC staining was performed as described previously [15] . Briefly, on the 7th day after surgery, the mice were anesthetized and decapitated. Brain slices were stained with 2% TTC (Catalog No. BCBW4269, Sigma, USA) for 15 min at 37°C in the dark. The normal tissue was stained red and the infarcted tissue was stained white. Infarct volume ratio (%)= V1/V2×100%, V1= $\sum$S1×d,V2= $\sum$S2×D (S1: infarct area of each section; S2: total area of each section; d: thickness of each piece was 1 mm).

Quantitative PCR

Total RNA was extracted using Trizol (Invitrogen, Carlsbad, CA, USA) and reverse transcribed to cDNA using cDNA synthesis kit (TAKARA, Japan). The reaction conditions were 95 °C for 10 min, followed by 40 cycles at 95 °C for 15 s and 60 °C for 60 s. The primers were purchased from SANGON Biotech (Shanghai, China) (Table 1). The expression of target genes was calculated using $2^{-\Delta\Delta CT}$ method, with glyceraldehyde 3-phosphate dehydrogenase (GAPDH) as internal control.

Immunofluorescent assay

The brains were removed from mice and fixed in 4% paraformaldehyde at 4℃ for 24 h. Brain tissues were treated with 30% sucrose solution for 72 h for dehydration and cut into slices (20 μm thick).

Sections were blocked with 5% BSA solution with 0.3% Triton X-100 in PBS (PBST) (Solarbio, Beijing, China) at room temperature for 1 h and then incubated with primary antibodies at 4℃ overnight. After washing with PBST, the sections were incubated with specific fluorescent secondary antibodies for 1 h at room temperature. The sections were observed under confocal microscope.

Evaluation of brain water content

Brain water content was measured with wet-dry weight method [20]. Mice were euthanized and the brains were removed carefully and quickly. The wet weight (WW) was measured after removing olfactory bulbs, cerebellum and pons. Subsequently, dry weight (DW) was measured after the brains were put in an oven at 110℃ for 6 h. Brain water content was evaluated by formula: WC = (WW−DW)/WW×100%.

Modified Neurological function score (mNSS)

Based on motor, sensory, reflex, and balance tests, neurological function was evaluated at 1 d, 3 d, 5 d and 1 w after stroke with modified Neurological Severity Scores (mNSS) as previously described [15]. Total mNSS score were 18 points, and the higher the score, the more severe neurological impairment.

Morris water maze test

Morris water maze test was performed to assess cognition function including learning and memory ability as previously described [18]. Briefly, mice were trained on three trials one day for three consecutive days before MCAO, and the experiments were carried out 31-34 d after MCAO surgery. Each mouse was trained 4 times a day with an interval of 10-15 min for 3 consecutive days. The time spent to reach the platform was recorded. The memory test was performed on 34 day to record the time of mice in the target quadrant (the quadrant where the platform was originally placed), the number of times of entering quadrant platform and total distance of swimming in 1 min.

Open field test.

Open field test was performed to evaluate the state of depression 28 days after stroke as previously described [21]. Briefly, the equipment was mainly composed of a square open box of 50cm×50cm× 50cm and was divided into peripheral area and central area. A video monitor was placed above the open field equipment to record the frequency and residence time of mice entering the central region. One week before the experiment, mice were placed in the behavioral test room for 3-5 min every day to eliminate the fear of the environment and the experimenter. At the beginning of the experiment, mice were gently placed into the open field from the edge, allowing them to explore freely in the open field for 5 min. the activity time and entry times in the central area of the open field were recorded.

Elevated plus maze

Elevated plus maze test was performed 29 days after stroke to evaluate anti-anxiety behavior by using the contradictory tendency of mice to explore new environment and the fear of the open arm hanging

high as previously described [22]. Briefly, the elevated cross maze consisted of two open arms with 50cm long and 10cm wide and closed arms. The four arms were connected by a central platform with a 10cm×10cm open part. The mice were placed on one side of the maze with open arms at the beginning of the experiment, and each animal was placed in the same position thereafter. The number of entries and the time spent in each arm were recorded for 5 min.

ELISA

Soluble CX3CL1 was detected by using ELISA kit (R&D Systems, Stillwater, MN, USA) following the manufacturer's instructions.

Statistical analysis

Data were shown as mean ± standard error of the mean (SEM) and analyzed by using GraphPad Prism software 8.1.0 (La Jolla, CA, USA). Data were tested for normal distribution using Kolmogorov-Smirnov test. Continuous variables with normal distributions were analyzed with Student's t test, non-normal distributions data were analyzed with Mann-Whitney test. One-way ANOVA was applied to compare the differences among multiple groups, followed by post hoc Bonferroni test for pairwise comparison.

Table 1 PCR primers sequences of different gene fragments.

Name	Primer
GAPDH	Forward: 5'- GCCAAGGCTGTGGGCAAGGT-3'
	Reverse: 5'-TCTCCAGGCGGCACGTCAGA-3'
iNOS	Forward:5'-CAGCTGGGCTGTACAAACCTT-3'
	Reverse:5'-CATTGGAAGTGAAGCGTTTCG-3'
TNF-α	Forward:5'-TGTGCTCAGAGCTTTCAACAA-3'
	Reverse: 5'-CTTGATGGTGGTGCATGAGA-3'
IL-1β	Forward: 5'-AAGCCTCGTGC TGTCGGACC-3'
	Reverse: 5'-TGAGGCCCAAGGCCACAGGT-3'
IL-10	Forward:5'-GGCATGAGGATCAGCAGGGGC-3'
	Reverse:5'-TGGCTGAAGGCAGTCCGCAG-3'
CD163	Forward: 5'-GGGAAGAGTGGAGCTCAAGA-3'
	Reverse: 5'-ACCAGCTCCTTTCCCAAAAT-3'
VEGF	Forward: 5'-GGGGAGCAAGCAAGGCCAGG-3'
	Reverse: 5'-TCTCTGCCTCCGTGAGGGGC-3'

Results

Tat-CX3CL1 (357-395aa) reduced ischemic brain injury and improved neurobehavioral function after stroke.

TTC staining was used to detect the effects of Tat-CX3CL1 (357-395aa) on the volume of cerebral infarction at the time point of 7d after cerebral infarction. Compared to I/R group and DMSO group, Tat-CX3CL1 (357-395aa) at 5 μg/μL and 10 μg/μL significantly reduced tissue loss caused by stroke (P<0.001, Fig. 1A, B), which was dose-dependent, so 10 ug/uL concentration of Tat-CX3CL1 (357-395aa) was selected for subsequent experiments. Meanwhile, Tat-CX3CL1 (357-395aa) improved mNSS scores at I/R 1d and 3d significantly (P<0.05, Fig. 1E).

Tat-CX3CL1 (357-395aa) regulated microglia M1 to M2 phenotype polarization shift in the acute stroke phase.

To explore the potential function of Tat-CX3CL1 (357-395aa) in ischemic stroke, we first detected the expression of M1/M2 type inflammatory factors at different time points after ischemia/reperfusion. The results showed that TNF-α (microglia M1 type inflammatory factors) was increased at 6 h after stroke and peaked at 24 h (Supplemental Fig.2B), while the levels of other cytokines including iNOS and IL-1β also peaked at 24 h after stroke (Supplemental Fig.2A, C). However, the levels of M2 type inflammatory factors (CD-163, IL-10, and VEGF) were decreased at 3 h after stroke and kept stable to 24 h (Supplemental Fig. 2D-F). CD163 and IL-10 levels were increased from 48 h after stroke (Supplemental Fig.2D, E). Therefore, we selected 24 h time point to investigate microglia polarization.

PCR analysis of M1 and M2 type cytokines production showed that Tat-CX3CL1 (357-395aa) inhibited the production of proinflammatory factors (iNOS, TNF-α, and IL-1β) related to M1 type (Fig. 2A-C), and increased the level of anti-inflammatory factors (IL-10, CD163, and VEGF) related to M2 type at 24 h after stroke (Fig. 2D-F). Immunofluorescence assay of M1-type microglia (Iba1 and CD68 double staining) in the cortex and striatum around the infarct area after 24 h reperfusion showed that the number of M1 microglia decreased significantly in Tat-CX3CL1 (357-395aa) group not only in cortex region but also in striatum region (Fig. 3A-D). These data suggest the Tat-CX3CL1 (357-395aa) may affect the microglia M1/M2 phenotype switch during ischemic stroke.

Tat-CX3CL1 (357-395aa) inhibited the generation of sCX3CL1 and improved brain edema.

CX3CL1 is localized on neurons and has membrane-anchored CX3CL1 (mCX3CL1) and soluble CX3CL1 (sCX3CL1) isoforms [29]. mCX3CL1 is cleaved into sCX3CL1 by the disintegrin and metalloproteinase (ADAM10 and ADAM17) [30, 31]. To elucidate the mechanism by which Tat-CX3CL1 (357-395) regulated microglia polarization transformation, we firstly tested the effect of Tat-CX3CL1 (357-395) on the generation of sCX3CL1 and found that Tat-CX3CL1 (357-395) inhibited the formation of sCX3CL1 (Fig. 2G). Meanwhile, we applied ADAM17 inhibitor GW280264x and found that GW280264x not only inhibited the expression of proinflammatory cytokines including iNOS, TNF-α, and IL-1β and facilitated the

expression of anti-inflammatory cytokines including CD-163, IL-10, and VEGF (Fig. 4A-F), but also reduced the production of sCX3CL1 (Fig. 2H). In addition, we found that Tat-CX3CL1 (357-395aa) reduced cerebral edema after infarction (Fig 1C, D).

Tat-CX3CL1 (357-395aa) promoted functional recovery of cognitive dysfunction after stroke by improving the integrity of myelinated fibers.

White matter injury after stroke is associated with cognitive deficits, neuroinflammation, demyelination, and the degeneration of axons [32-34]. To explore whether Tat-CX3CL1 (357-395aa) could improve cognitive dysfunction, we performed Morris water maze test and found that Tat-CX3CL1 (357-395aa) reduced the escape latency and extended the time spent in the target quadrant, but did not affect swimming speed (Fig. 6A-D). Next, we evaluated whether Tat-CX3CL1 (357-395aa) could improve white matter integrity in stroke. Dual staining for SMI32 (a marker of demyelinated axons) and myelin basic protein (MBP, a major myelin protein) showed the lesion in white matter (Fig. 5A, B) was alleviated. The immunofluorescence intensity of MBP staining was decreased in corpus callosum (CC) and cortex regions at 35 d after MCAO (Fig 5C, 5D). However, Tat-CX3CL1 (357-395aa) increased the loss of myelin protein significantly. SMI32/MBP ratio was used to analyze the repair of myelin sheath and white matter. The results showed that the SMI32/MBP ratio in corpus callosum (CC) and cortex regions was increased significantly in I/R and DMSO groups compared to sham group, but was decreased in Tat-CX3CL1 (357-395aa) group compared to I/R and MDSO group (Fig. 5E, F).

Tat-CX3CL1 (357-395aa) improved post-stroke anxiety and depression.

Post-stroke depression and anxiety exacerbate cognitive dysfunction, we suspect the underlying mechanism might be related to microglia polarization. We observed the anxiety-like behavior and depression state using open field test and elevated plus maze. As shown in Fig. 7, compared to I/R group and DMSO group, the number of entering the open arm and dwell time increased significantly in Tat-CX3CL1 (357-395aa) mice.

Additionally, Tat-CX3CL1 (357-395aa) significantly increased the frequency of mice entering the central area and the activity time in the central area of open field. These results suggested that Tat-CX3CL1 (357-395aa) improved post-stroke anxiety and depression.

Discussion

In present study, we demonstrated protective effects of Tat-CX3CL1 (357-395aa) on stroke by blocking the interaction of PSD-93 and CX3CL1 and reducing the production of soluble CX3CL1, resulting in inhibiting the communication between neuron and microglia. We found that the peaks for the expression of pro-inflammatory cytokines (M1 like) and anti-inflammatory cytokines (M2 like) were different. Thus we proposed that the peptide Tat-CX3CL1 (357-395aa) reduced pro-inflammatory cytokines secretion while promoted anti-inflammatory cytokines expression in acute ischemia-reperfusion due to M1 and M2 phenotypic polarization shift (Fig. 8). Furthermore, the peptide Tat-CX3CL1 (357-395aa) diminished

neurological impairment and improved long-term cognitive dysfunction after stroke. Collectively, these data support the beneficial effects of Tat-CX3CL1 (357-395aa) and the peptide may be a therapeutic agent for ischemic stroke.

Accumulating evidences showed that microglia are polarized into different states within hours following the onset of stroke. Differential polarization of microglia including classic pro-inflammatory type (M1-like) and alternative protective type (M2-like) is activated at different stage, and exerts detrimental or beneficial potential role [10, 36, 37]. However, molecular mechanism underlying microglia polarization during stroke remains to be elucidated.

In this study, we reported M1/M2-like microglia activation at different stage after stroke. M1-like microglia was activated at 6 h after stoke and peaked at 24 h and then persisted several days, consistent with the peak expression of sCX3CL1[17], which indicates that splicing into sCX3CL1 promotes M1-like microglia activation. Conversely, M2-like microglia was suppressed at 24 h following stroke. Meanwhile, we found that Tat-CX3CL1 (357-395aa) facilitated microglia polarization from M1 to M2 phenotype by inhibiting M1-phenotype cytokines (iNOS, TNF-α, and IL-1β) and promoting M2-phenotype cytokines (CD-163, IL-10, and VEGF) at 24 h after stroke.

Previously we reported that PSD-93 bound to CX3CL1 and the binding amino acid sequences were located at 420-535 amino acids of PSD-93 and 357-395 amino acids of CX3CL1, and we designed the peptide Tat-CX3CL1 (357-395aa) to block the binding of PSD-93 and CX3CL1 [17]. CX3CL1/CX3CR1 signaling is crucial for microglia-neuron cross-talk [24-28,38]. In addition, PSD-93 combined with CX3CL1 and facilitated the generation of soluble form of CX3CL1, which then bound to CX3CR1 receptor expressed on microglia [17]. We found that Tat-CX3CL1 (357-395aa) reduced the release of soluble CX3CL1 and inhibited pro-inflammatory type (M1-like) cytokines, suggesting that Tat-CX3CL1 (357-395aa) suppressed soluble CX3CL1 expression and inhibited CX3CL1/CX3CR1 signaling.

Previous study revealed that CX3CL1-CX3CR1 signaling regulated synaptic plasticity and cognitive function [39-42]. Ischemic stroke impacts not only gray matter but also white matter and induces cognitive deficits in memory and learning. Furthermore, the incidence of post-stroke anxiety and depression is about 36.7% within 2 weeks after stroke [43, 44]. In this study, we showed that Tat-CX3CL1 (357-395aa) promoted white matter repair and cognitive improvement. Additionally, Tat-CX3CL1 (357-395aa) showed beneficial potential role on post-stroke anxiety and depression. These results suggest that the inhibition of microglial polarization in acute stage of ischemic infarction will be beneficial for the rehabilitation of nerve function in the later stage, and Tat-CX3CL1 (357-395aa) is an attractive agent for stroke therapy.

Conclusion

Our findings indicated that Tat-CX3CL1 (357-395aa) inhibited the generation of soluble CX3CL1 and promoted M2 type microglia polarization, and exerted neuroprotective effects in mouse ischemic stroke model. The peptide Tat-CX3CL1 (357-395aa) might be a potential therapeutic agent for ischemic stroke.

Abbreviations

ADAM, A distintegrin and metalloproteinase; BD, Binding-domain; CX3CL1, Chemokine C-X3-C-Motif ligand 1; IL-1β, Interleukin 1β; MCAO, Middle cerebral artery occlusion; NMDAR, N-methyl-D-aspartic acid receptor; PSD-93, Postsynaptic densitries-93; TNF-α, Tumor necrosis factor-alpha; MCAO, middle cerebral artery occlusion model; mNSS, modified neurological function score; TTC, triphenyl tetrazolium chloride; I/R, ischemia/reperfusion; BBB, blood-brain barrier.

Declarations

Acknowledgements

Not applicable.

Author contributions

Qingxiu Zhang designed and performed the experiments, and drafted the manuscript. Yun Xu designed the experiments, interpreted the data and edited the manuscript. Liangqun Rong interpreted the data and edited the manuscript. Xiaowei Cao conducted the experiments, analyzed the data, and drafted the manuscript. Hui Yang performed the experiments and analyzed the data. Liping Kong, Junjun shan and Shiying Lou conducted the experiments and analyzed the data. Xiaomei Liu conceived the experiments, interpreted the data and edited the manuscript. All authors approved the manuscript before submission.

Ethics approval and consent to participate

All animal experiments were performed at Xuzhou Medical University according to Animal Care and Use Committee of Xuzhou Medical University. Mice were euthanized by cervical dislocation. Ethics approval reference number was 201702w012.

Consent for publication

Not applicable.

Availability of data and materials

All data are available upon reasonable request to correspondence author.

Competing interests

The authors declare that they have no competing interests.

Funding

This study was supported by the National Natural Science Foundation of China (No. 81671149, 82071304, and 81971179), the Natural Science Foundation of Jiangsu Province (No.BK20161167, and

BK20191463), Subject of Xuzhou Science and Technology Bureau (KC19167, KC16SS081 and KC17115), and Youth Project of Health Department of Jiangsu Province (Q201618).

References

1. Global, regional, and national burden of stroke, 1990-2016: a systematic analysis for the Global Burden of Disease Study 2016. Lancet Neurol 2019, 18:439-58.

2. Jin R, Liu L, Zhang S, Nanda A, Li G: Role of inflammation and its mediators in acute ischemic stroke. J Cardiovasc Transl Res 2013, 6:834-51.

3. Rong R, Yang H, Rong L, Wei X, Li Q, Liu X, Gao H, Xu Y, Zhang Q: Proteomic analysis of PSD-93 knockout mice following the induction of ischemic cerebral injury. Neurotoxicology 2016, 53:1-11.

4. Zhang M, Li Q, Chen L, Li J, Zhang X, Chen X, Zhang Q, Shao Y, Xu Y: PSD-93 deletion inhibits Fyn-mediated phosphorylation of NR2B and protects against focal cerebral ischemia. Neurobiol Dis 2014, 68:104-11.

5. Ma Y, Wang J, Wang Y, Yang GY: The biphasic function of microglia in ischemic stroke. Prog Neurobiol 2017, 157:247-72.

6. Wang J, Xing H, Wan L, Jiang X, Wang C, Wu Y: Treatment targets for M2 microglia polarization in ischemic stroke. Biomed Pharmacother 2018, 105:518-25.

7. Gelderblom M, Leypoldt F, Steinbach K, Behrens D, Choe CU, Siler DA, Arumugam TV, Orthey E, Gerloff C, Tolosa E, Magnus T: Temporal and spatial dynamics of cerebral immune cell accumulation in stroke. Stroke 2009, 40:1849-57.

8. Hu X, Leak RK, Shi Y, Suenaga J, Gao Y, Zheng P, Chen J: Microglial and macrophage polarization—new prospects for brain repair. Nat Rev Neurol 2015, 11:56-64.

9. Gülke E, Gelderblom M, Magnus T: Danger signals in stroke and their role on microglia activation after ischemia. Ther Adv Neurol Disord 2018, 11:1756286418774254.

10. Hu X, Li P, Guo Y, Wang H, Leak RK, Chen S, Gao Y, Chen J: Microglia/macrophage polarization dynamics reveal novel mechanism of injury expansion after focal cerebral ischemia. Stroke 2012, 43:3063-70.

11. Rayasam A, Hsu M, Kijak JA, Kissel L, Hernandez G, Sandor M, Fabry Z: Immune responses in stroke: how the immune system contributes to damage and healing after stroke and how this knowledge could be translated to better cures? Immunology 2018, 154:363-76.

12. Liu X, Liu J, Zhao S, Zhang H, Cai W, Cai M, Ji X, Leak RK, Gao Y, Chen J, Hu X: Interleukin-4 Is Essential for Microglia/Macrophage M2 Polarization and Long-Term Recovery After Cerebral Ischemia.

Stroke 2016, 47:498-504.

13. Qin C, Zhou LQ, Ma XT, Hu ZW, Yang S, Chen M, Bosco DB, Wu LJ, Tian DS: Dual Functions of Microglia in Ischemic Stroke. Neurosci Bull 2019, 35:921-33.

14. Fumagalli M, Lombardi M, Gressens P, Verderio C: How to reprogram microglia toward beneficial functions. Glia 2018, 66:2531-49.

15. Zhang Q, Yang H, Gao H, Liu X, Li Q, Rong R, Liu Z, Wei XE, Kong L, Xu Y, Rong L: PSD-93 Interacts with SynGAP and Promotes SynGAP Ubiquitination and Ischemic Brain Injury in Mice. Transl Stroke Res 2020, 11:1137-47.

16. Zhang Q, Cheng H, Rong R, Yang H, Ji Q, Li Q, Rong L, Hu G, Xu Y: The Effect of PSD-93 Deficiency on the Expression of Early Inflammatory Cytokines Induced by Ischemic Brain Injury. Cell Biochem Biophys 2015, 73:695-700.

17. Zhang Q, He L, Chen M, Yang H, Cao X, Liu X, Hao Q, Chen Z, Liu T, Wei XE, Rong L: PSD-93 mediates the crosstalk between neuron and microglia and facilitates acute ischemic stroke injury by binding to CX3CL1. J Neurochem 2021.

18. Zhang Q, Zhu W, Xu F, Dai X, Shi L, Cai W, Mu H, Hitchens TK, Foley LM, Liu X, et al: The interleukin-4/PPARγ signaling axis promotes oligodendrocyte differentiation and remyelination after brain injury. PLoS Biol 2019, 17:e3000330.

19. Dreymueller D, Martin C, Kogel T, Pruessmeyer J, Hess FM, Horiuchi K, Uhlig S, Ludwig A: Lung endothelial ADAM17 regulates the acute inflammatory response to lipopolysaccharide. EMBO Mol Med 2012, 4:412-23.

20. Qi W, Cao D, Li Y, Peng A, Wang Y, Gao K, Tao C, Wu Y: Atorvastatin ameliorates early brain injury through inhibition of apoptosis and ER stress in a rat model of subarachnoid hemorrhage. Biosci Rep 2018, 38.

21. Donatti AF, Soriano RN, Leite-Panissi CR, Branco LG, de Souza AS: Anxiolytic-like effect of hydrogen sulfide (H(2)S) in rats exposed and re-exposed to the elevated plus-maze and open field tests. Neurosci Lett 2017, 642:77-85.

22. Kraeuter AK, Guest PC, Sarnyai Z: The Elevated Plus Maze Test for Measuring Anxiety-Like Behavior in Rodents. Methods Mol Biol 2019, 1916:69-74.

23. Laing JM, Smith CC, Aurelian L: Multi-targeted neuroprotection by the HSV-2 gene ICP10PK includes robust bystander activity through PI3-K/Akt and/or MEK/ERK-dependent neuronal release of vascular endothelial growth factor and fractalkine. J Neurochem 2010, 112:662-76.

24. Febinger HY, Thomasy HE, Pavlova MN, Ringgold KM, Barf PR, George AM, Grillo JN, Bachstetter AD, Garcia JA, Cardona AE, et al: Time-dependent effects of CX3CR1 in a mouse model of mild traumatic brain injury. J Neuroinflammation 2015, 12:154.

25. Lee S, Xu G, Jay TR, Bhatta S, Kim KW, Jung S, Landreth GE, Ransohoff RM, Lamb BT: Opposing effects of membrane-anchored CX3CL1 on amyloid and tau pathologies via the p38 MAPK pathway. J Neurosci 2014, 34:12538-46.

26. Pabon MM, Bachstetter AD, Hudson CE, Gemma C, Bickford PC: CX3CL1 reduces neurotoxicity and microglial activation in a rat model of Parkinson's disease. J Neuroinflammation 2011, 8:9.

27. Shan S, Hong-Min T, Yi F, Jun-Peng G, Yue F, Yan-Hong T, Yun-Ke Y, Wen-Wei L, Xiang-Yu W, Jun M, et al: New evidences for fractalkine/CX3CL1 involved in substantia nigral microglial activation and behavioral changes in a rat model of Parkinson's disease. Neurobiol Aging 2011, 32:443-58.

28. Mizuno T, Kawanokuchi J, Numata K, Suzumura A: Production and neuroprotective functions of fractalkine in the central nervous system. Brain Res 2003, 979:65-70.

29. Bajetto A, Bonavia R, Barbero S, Schettini G: Characterization of chemokines and their receptors in the central nervous system: physiopathological implications. J Neurochem 2002, 82:1311-29.

30. Clark AK, Yip PK, Grist J, Gentry C, Staniland AA, Marchand F, Dehvari M, Wotherspoon G, Winter J, Ullah J, et al: Inhibition of spinal microglial cathepsin S for the reversal of neuropathic pain. Proc Natl Acad Sci U S A 2007, 104:10655-60.

31. Garton KJ, Gough PJ, Blobel CP, Murphy G, Greaves DR, Dempsey PJ, Raines EW: Tumor necrosis factor-alpha-converting enzyme (ADAM17) mediates the cleavage and shedding of fractalkine (CX3CL1). J Biol Chem 2001, 276:37993-8001.

32. Rosenzweig S, Carmichael ST: The axon-glia unit in white matter stroke: mechanisms of damage and recovery. Brain Res 2015, 1623:123-34.

33. Shi H, Hu X, Leak RK, Shi Y, An C, Suenaga J, Chen J, Gao Y: Demyelination as a rational therapeutic target for ischemic or traumatic brain injury. Exp Neurol 2015, 272:17-25.

34. Wang Y, Liu G, Hong D, Chen F, Ji X, Cao G: White matter injury in ischemic stroke. Prog Neurobiol 2016, 141:45-60.

35. Liu Y, Wu C, Hou Z, Fu X, Yuan L, Sun S, Zhang H, Yang D, Yao X, Yang J: Pseudoginsenoside-F11 Accelerates Microglial Phagocytosis of Myelin Debris and Attenuates Cerebral Ischemic Injury Through Complement Receptor 3. Neuroscience 2020, 426:33-49.

36. Mabuchi T, Kitagawa K, Ohtsuki T, Kuwabara K, Yagita Y, Yanagihara T, Hori M, Matsumoto M: Contribution of microglia/macrophages to expansion of infarction and response of oligodendrocytes

after focal cerebral ischemia in rats. Stroke 2000, 31:1735-43.

37. Lakhan SE, Kirchgessner A, Hofer M: Inflammatory mechanisms in ischemic stroke: therapeutic approaches. J Transl Med 2009, 7:97.

38. Luo P, Chu SF, Zhang Z, Xia CY, Chen NH: Fractalkine/CX3CR1 is involved in the cross-talk between neuron and glia in neurological diseases. Brain Res Bull 2019, 146:12-21.

39. Meucci O, Fatatis A, Simen AA, Miller RJ: Expression of CX3CR1 chemokine receptors on neurons and their role in neuronal survival. Proc Natl Acad Sci U S A 2000, 97:8075-80.

40. Ragozzino D, Di Angelantonio S, Trettel F, Bertollini C, Maggi L, Gross C, Charo IF, Limatola C, Eusebi F: Chemokine fractalkine/CX3CL1 negatively modulates active glutamatergic synapses in rat hippocampal neurons. J Neurosci 2006, 26:10488-98.

41. Deiva K, Geeraerts T, Salim H, Leclerc P, Héry C, Hugel B, Freyssinet JM, Tardieu M: Fractalkine reduces N-methyl-d-aspartate-induced calcium flux and apoptosis in human neurons through extracellular signal-regulated kinase activation. Eur J Neurosci 2004, 20:3222-32.

42. Limatola C, Lauro C, Catalano M, Ciotti MT, Bertollini C, Di Angelantonio S, Ragozzino D, Eusebi F: Chemokine CX3CL1 protects rat hippocampal neurons against glutamate-mediated excitotoxicity. J Neuroimmunol 2005, 166:19-28.

43. Pérez-Piñar M, Ayerbe L, González E, Mathur R, Foguet-Boreu Q, Ayis S: Anxiety disorders and risk of stroke: A systematic review and meta-analysis. Eur Psychiatry 2017, 41:102-08.

44. Rafsten L, Danielsson A, Sunnerhagen KS: Anxiety after stroke: A systematic review and meta-analysis. J Rehabil Med 2018, 50:769-78.

Figures

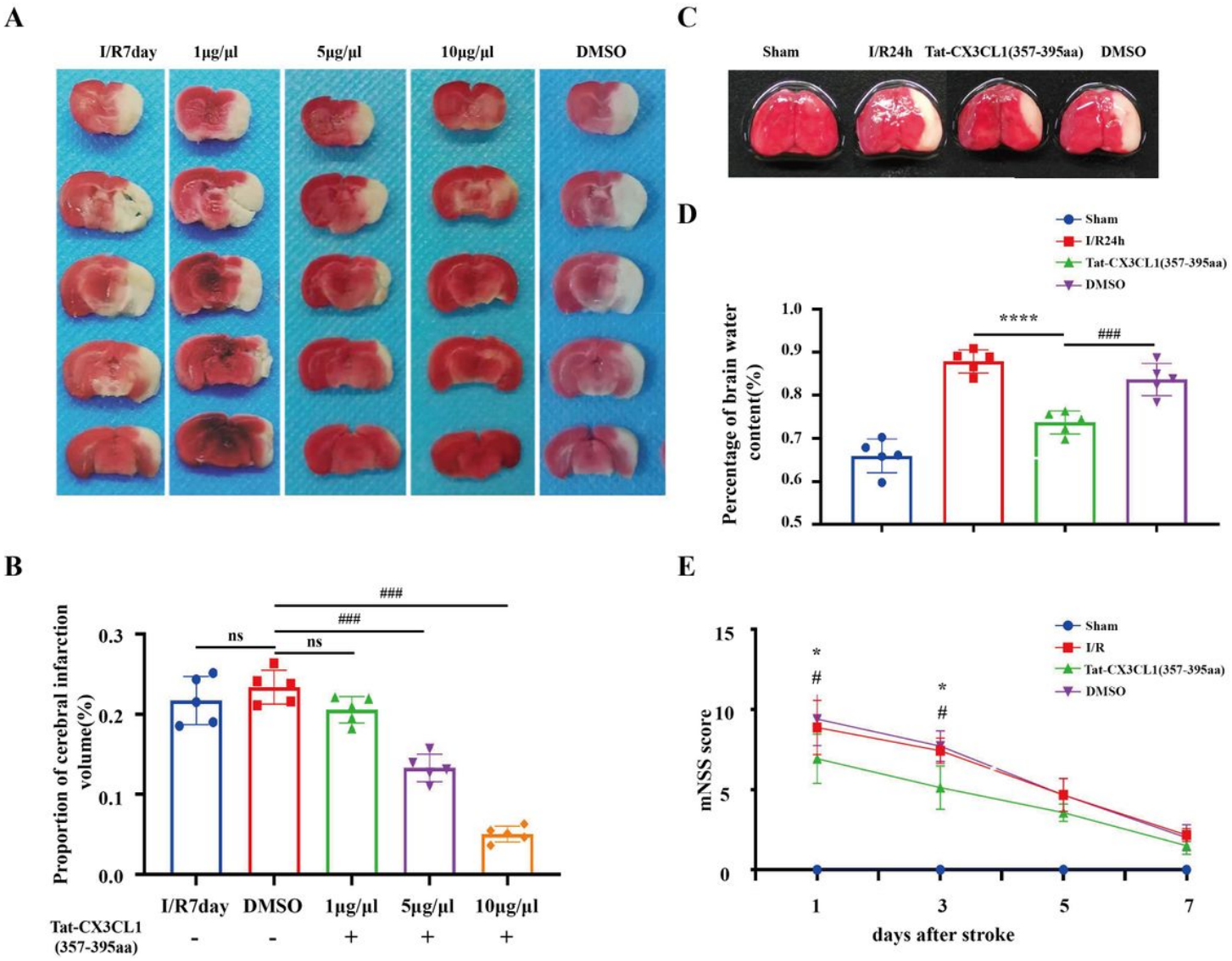

Figure 1

Tat-CX3CL1 (357-395aa) reduced infarct volume, brain edema and improved neurological function in mice after cerebral infarction. (A-B) TTC staining showed that Tat-CX3CL1 (357-395aa) reduced infarct volume. ###P<0.001, 5μg/μL Tat-CX3CL1 (357-395aa) group versus DMSO group; ###P<0.001, 10μg/μL Tat-CX3CL1 (357-395aa) group versus DMSO group, n=5. (C) TTC staining of the brains at R24h in each group. (D) Tat-CX3CL1 (357-395aa) reduced the water content of brain tissues after infarction. ****P<0.0001, Tat-CX3CL1 (357-395aa) group versus I/R group; ###P<0.001, Tat-CX3CL1 (357-395aa) group versus DMSO group, n=5. (E) mNSS scores showed a gradual improvement in neurological function after cerebral infarction in Tat-CX3CL1 (357-395aa) group. *P<0.05, Tat-CX3CL1 (357-395aa) group versus I/R group; #P<0.05, Tat-CX3CL1 (357-395aa) group versus DMSO group, n=8-17.

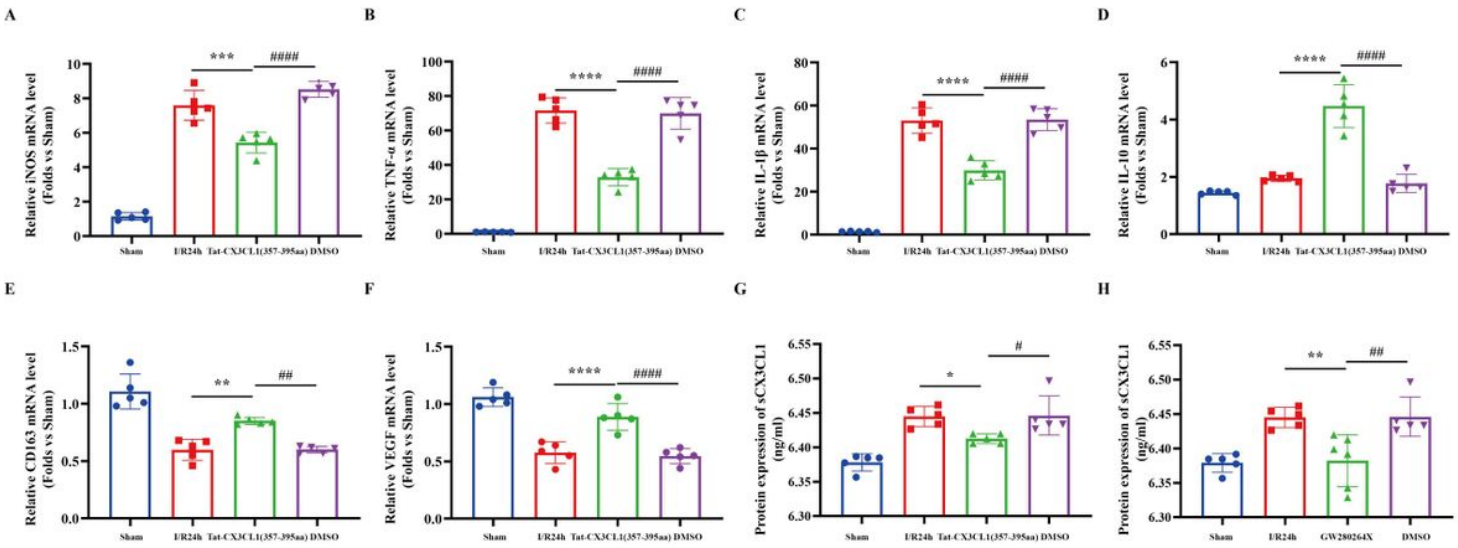

Figure 2

Effects of Tat-CX3CL1 (357-395aa) on phenotypic polarization of M1/M2 microglia at R24h. (A-C) Tat-CX3CL1 (357-395aa) reduced the expression of iNOS, TNF-α, and IL-1β. (D-F) Tat-CX3CL1 (357-395aa) increased the expression of IL-10, CD163 and VEGF. (G) Tat-CX3CL1 (357-395aa) at 10μg/μL concentration decreased the production of sCX3CL1 at 6h after stroke. (H) GW280264x at 1.5 ug/ul concentration inhibited the expression of sCX3CL1 at I/R 6h. *P < 0.05, **P < 0.01, ***P < 0.001, ****P < 0.0001, Tat - CX3CL1 (357-395aa) group versus I/R group; #P < 0.05, ##P < 0.01, ####P < 0.0001Tat-CX3CL1 (357-395aa) group versus DMSO group, n = 5.

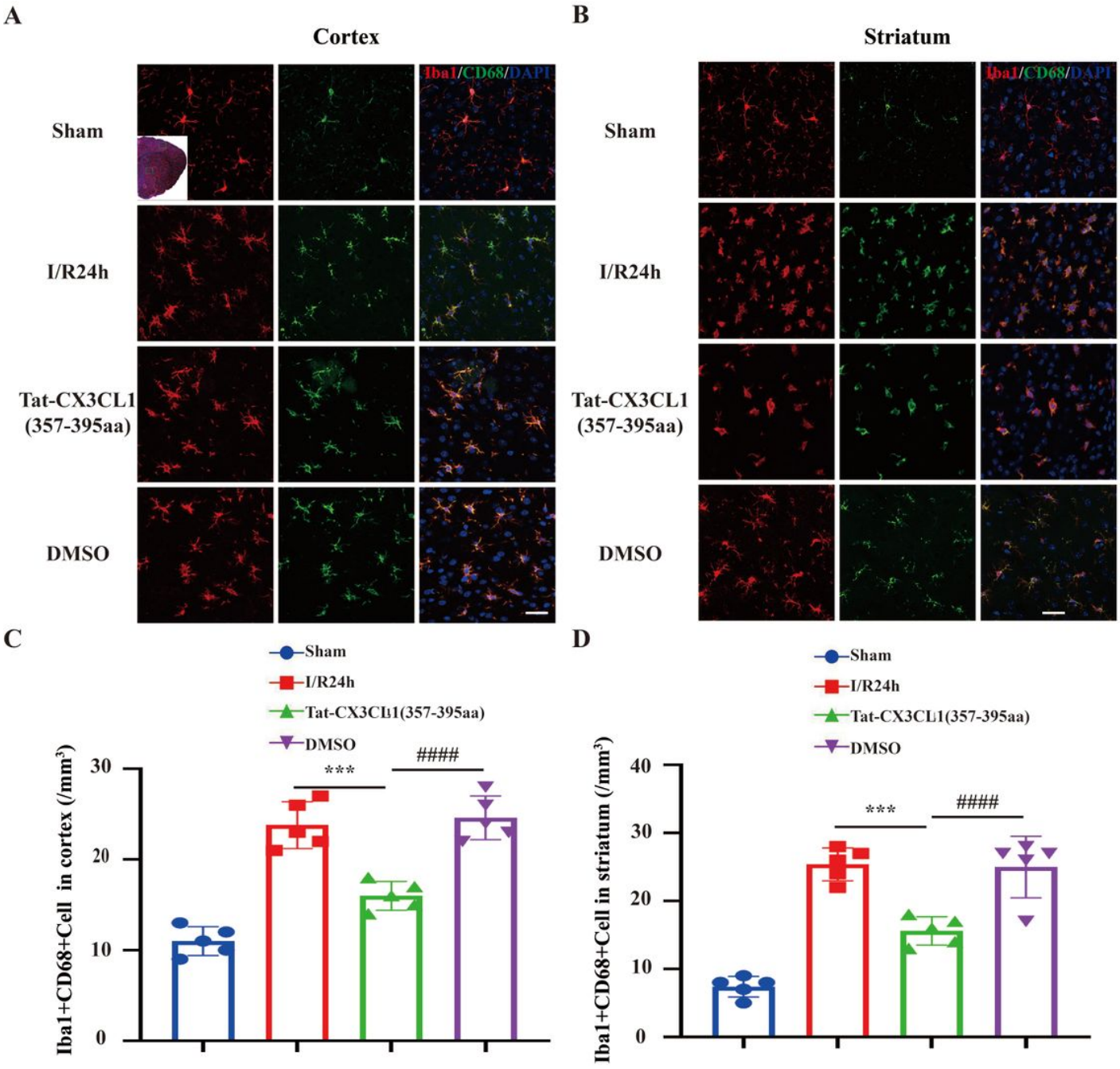

Figure 3

Tat-CX3CL1 (357-395aa) inhibited the polarization of M1-type microglia. (A, B) Representative images of Iba1 (red) and CD68 (green) immunostaining in cortex and striatum at 24 h after cerebral ischemia. Scale bar: 50μm. Selected areas were observed in cortex and striatum. (C, D) Quantification of the number of Iba1+ CD68+ cells in the peri-infarct areas of cortex and striatum. ***P < 0.001, Tat-CX3CL1 (357-395aa) group versus I/R group; ####P < 0.0001, Tat-CX3CL1 (357-395aa) group versus DMSO group, n=5.

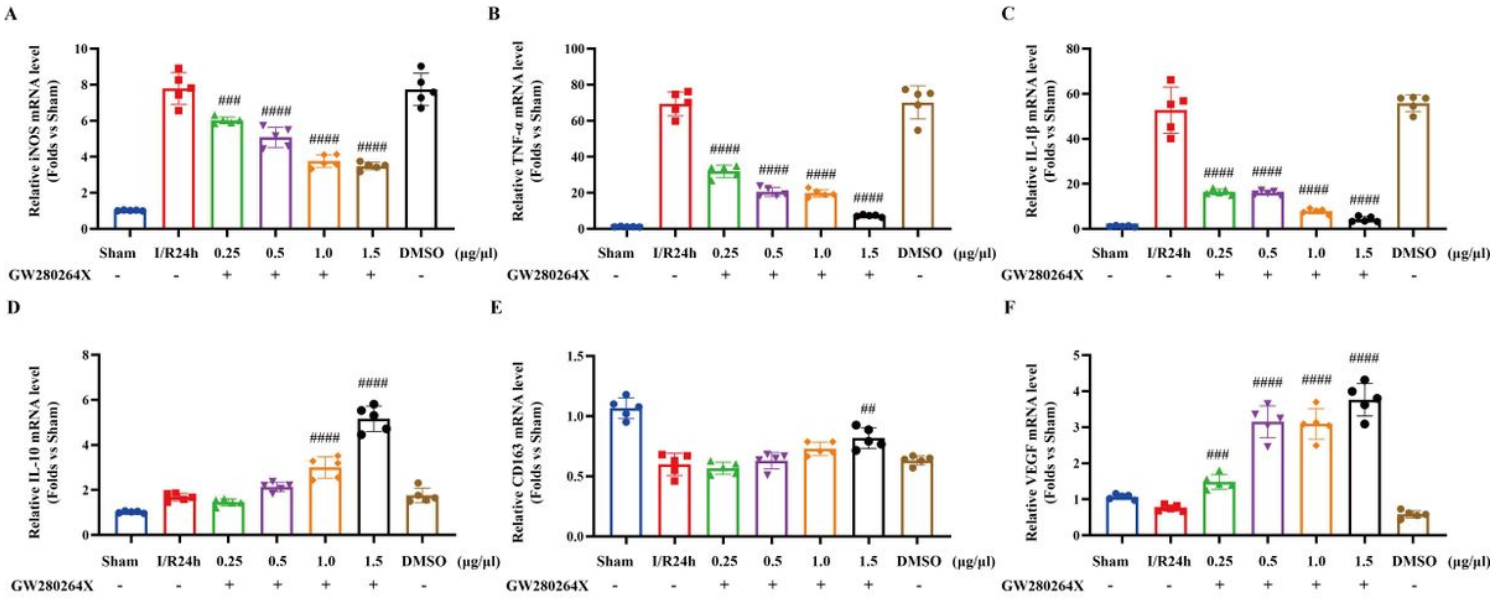

Figure 4

ADAM17 inhibitor GW280264x facilitated M1 to M2 phenotypic shift at 24 h after stroke. (A-C) GW280264x (0.25, 0.5, 1.0, 1.5 ug/ul) inhibited the expression of iNOS, TNF-α, IL-1β significantly. (D-F) GW280264x (0.25, 0.5, 1.0, 1.5 ug/ul) increased the expression of CD163, IL-10, and VEGF. ##P<0.01, ###P<0.001, ####P□0.0001, Tat-CX3CL1 (357-395aa) group versus DMSO group, n=5.

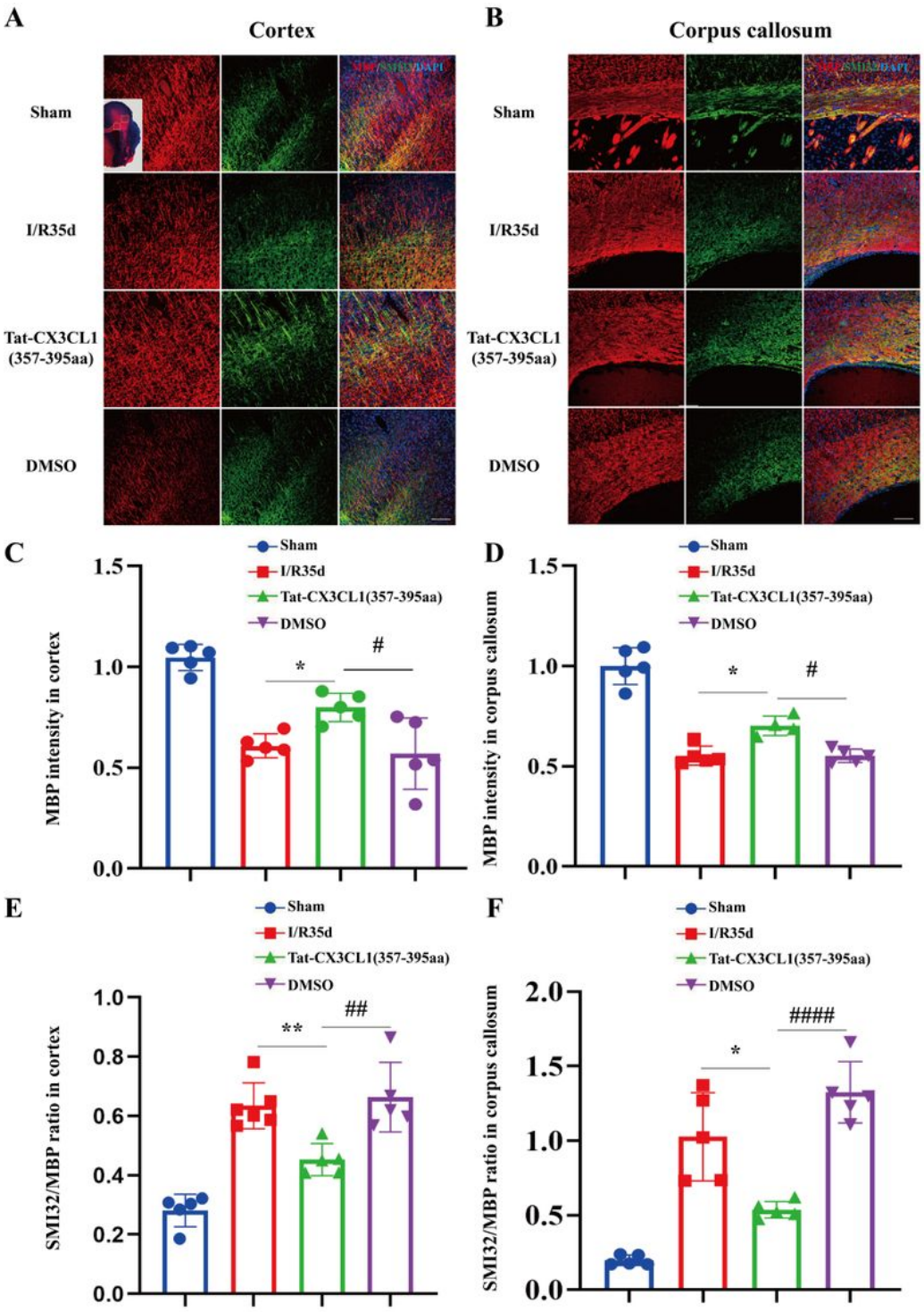

Figure 5

Tat-CX3CL1 (357-395aa) improved white matter injury followed stroke injury. Double immunostaining of MBP and SMI32 at 35 d after MCAO or sham operation. Representative images for MBP (red) and SMI32 (green) double immunostaining peri-infarct areas in cortex (A) and CC (B) from sham, I/R 35d group, DMSO group, and Tat-CX3CL1 (357-395aa) group. Selected areas were observed in cortex and striatum. The fluorescence intensity of MBP in cortex (C) and CC (D). The ratio of SMI32 to MBP

immunofluorescence intensity in cortex (E) and CC (F). Scale bar: 100 μm. n=5. *P < 0.05, **P < 0.01, Tat-CX3CL1 (357-395aa) group versus I/R group; #P<0.05, ##P<0.01, ####P<0.0001, Tat-CX3CL1 (357-395aa) group versus DMSO group.

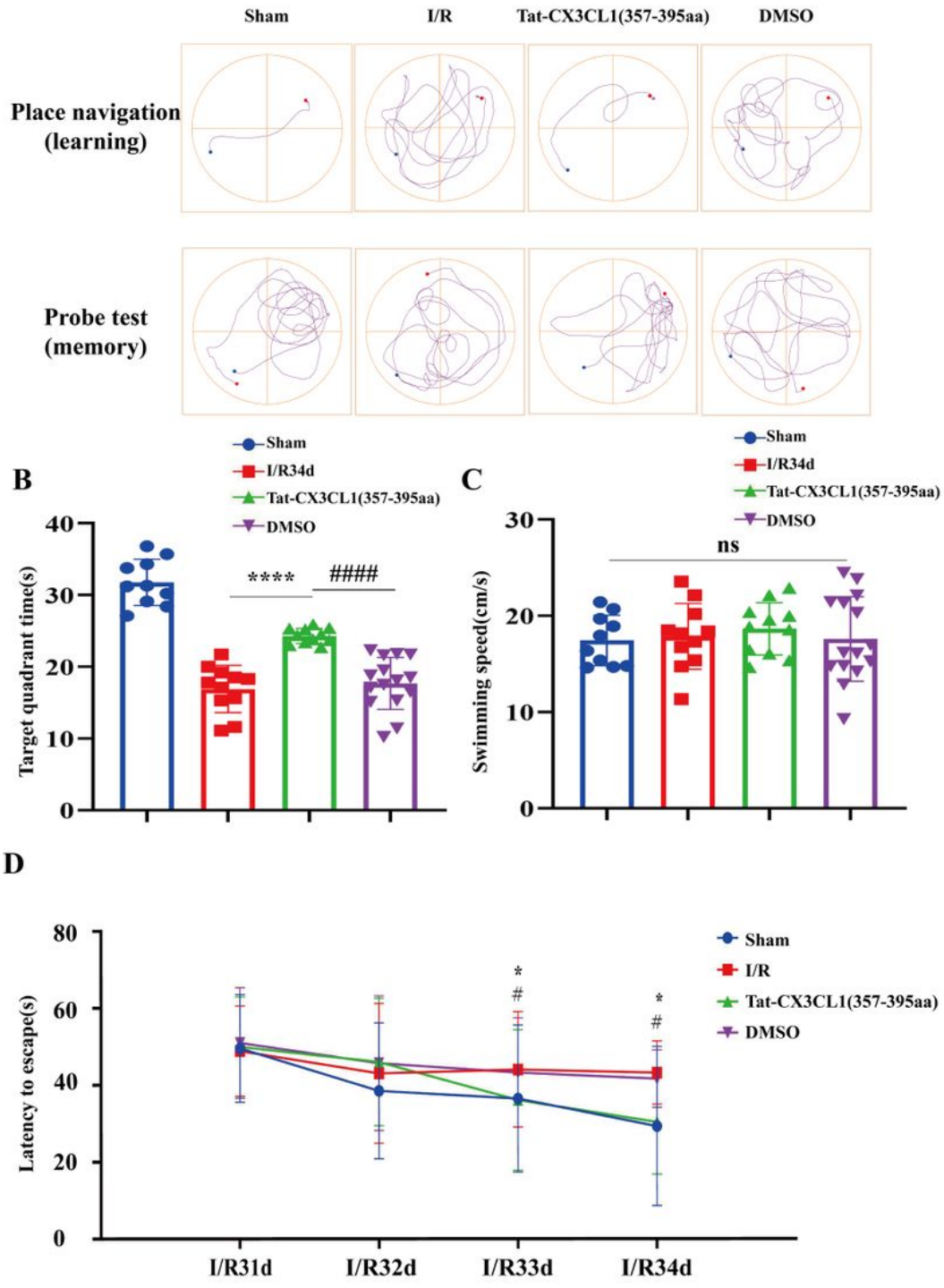

Figure 6

Tat-CX3CL1 (357-395aa) performed beneficial role in long-term cognitive function impairment after MCAO. Long-term cognitive function evaluated by Morris water maze test. (A) Representative images of

the swim paths in each group while the platform was present (learning phase) or removed (memory phase). n=10-15/group. (B) Tat-CX3CL1 (357-395aa) extended the time spent in the target quadrant (memory). (C) There was no change in swimming speed in each group. (D) Tat-CX3CL1 (357-395aa) reduced the escape latency in mice significantly (learning). *P < 0.05, ****P□0.0001, Tat-CX3CL1 (357-395aa) group versus I/R group; #P<0.05, ####P<0.0001, Tat-CX3CL1 (357-395aa) group versus DMSO group.

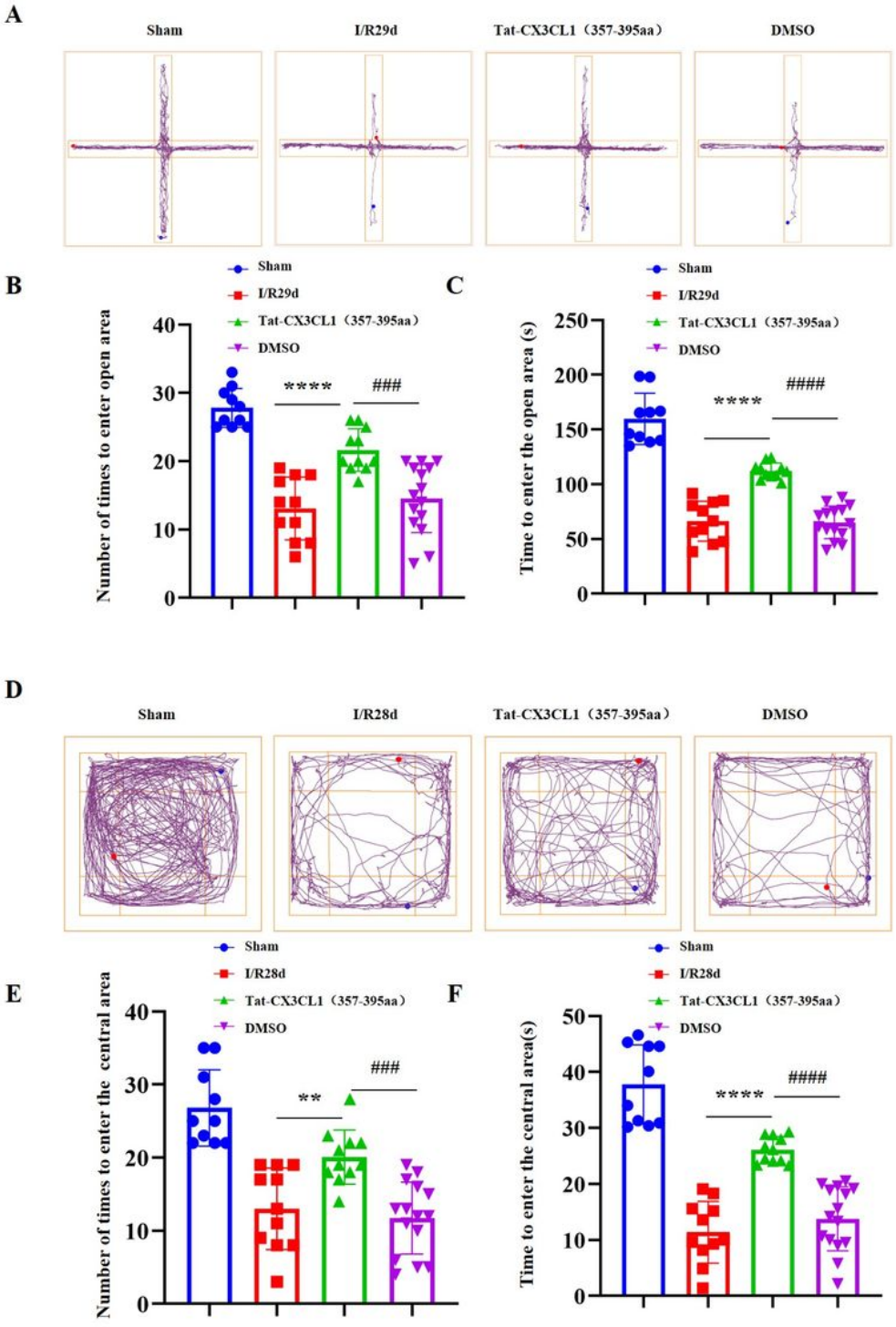

Figure 7

Tat-CX3CL1 (357-395aa) alleviated post-stroke anxiety and depression in mice. (A) Representative images of movement paths in elevated plus maze in each group. (B, C) Tat-CX3CL1 (357-395aa) increased the number of entering the open arm and the time spent on the open arm. (D) Representative images of movement paths in open field experiment. (E, F) Tat-CX3CL1 (357-395aa) increased the number and time of entering the central region. **P<0.01, ****P<0.0001, Tat-CX3CL1 (357-395aa) group versus I/R group; ###P<0.001, ####P<0.0001, Tat-CX3CL1 (357-395aa) group versus DMSO group, n=10-15.

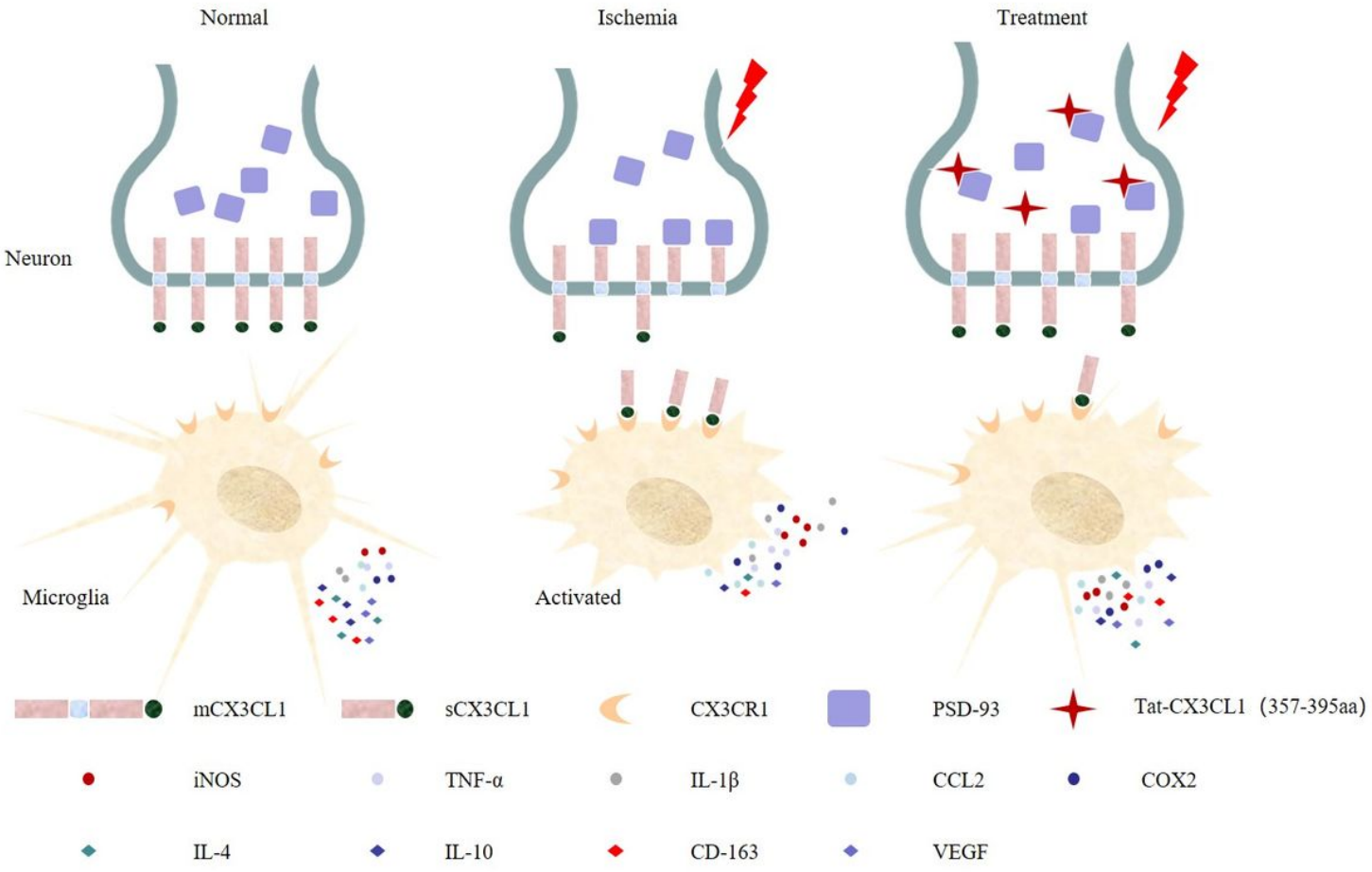

Figure 8

Schematic diagram of neuroprotective effects of Tat-CX3CL1 (357-395aa) during ischemic cerebral injury. Tat-CX3CL1 (357-395aa) blocked the combination of PSD-93 and CX3CL1, inhibited the generation of soluble CX3CL1, and promoted phenotypic polarization transformation of microglia from M1 type to M2 type.

Supplementary Files

This is a list of supplementary files associated with this preprint. Click to download.

- supplemental1.jpg

- supplemental2.jpg